Br J Dermatol 2024; **191**:949–963
https://doi.org/10.1093/bjd/ljae255
Advance access publication date: 15 June 2024

BJD
British Journal of Dermatology
Translational Research

Cytokeratin 17 expression is commonly observed in keratinocytic skin tumours and controls tissue homeostasis impacting human papillomavirus protein expression

Daniel Hasche[1], Martin Hufbauer[2], Ilona Braspenning-Wesch[1], Sonja Stephan[1], Steffi Silling[2], Gabriele Schmidt[3], Stephan Krieg[4], Alexander Kreuter[5] and Baki Akgül[2]

[1]Division of Viral Transformation Mechanisms, German Cancer Research Center (DKFZ), Heidelberg, Germany
[2]National Reference Center for Papilloma- and Polyomaviruses and Institute of Virology, University of Cologne, Medical Faculty and University Hospital Cologne, Cologne, Germany
[3]Light Microscopy Core Facility, German Cancer Research Center (DKFZ), Heidelberg, Germany
[4]Helmholtz-University Group Cell Plasticity and Epigenetic Remodeling, German Cancer Research Center (DKFZ) & Institute of Pathology, University Hospital, Heidelberg, Germany
[5]Department of Dermatology, Venereology and Allergology, Helios St. Elisabeth Hospital Oberhausen, University of Witten/Herdecke, Oberhausen, Germany

Correspondence: Baki Akgül. Email: baki.akguel@uk-koeln.de

Linked Article: Brito and O'Toole *Br J Dermatol* 2024; **191**:862–863.

Abstract

Background The structured expression of several keratins in the skin is associated with differentiation status of the epidermal layers, whereas other keratins are upregulated only during wound healing, in skin disorders and in cancers. One of these stress keratins, K17, is correlated with poor prognosis in various cancer types and its loss has been shown to decelerate tumour growth. K17 expression can also be detected in cutaneous squamous cell carcinomas, where ultraviolet irradiation and infection with cutaneous human papillomaviruses are important cofactors. It was previously reported that K17 is upregulated in papillomavirus (PV)-induced benign skin lesions in mice and induces an immunological status that is beneficial for tumour growth.

Objectives In order to investigate whether K17 upregulation is induced by PVs, we analysed K17 levels in skin tumour specimens of different animal models and humans.

Methods Various immunofluorescence stainings were performed to identify K17 expression as well as levels of E-cadherin, vimentin and CD271. Tissues were further analysed by polymerase chain reaction (PCR), quantitative (q)PCR and enzyme-linked immunosorbent assay to control for PV activity. K17 knockdown cells were generated and effects on viral life cycle were investigated by infection assays, qPCR and Western blotting.

Results We showed that K17 is commonly expressed in skin tumours and that its presence is not directly linked to viral oncoprotein expression. Rather, K17 expression seems to be a marker of epithelial differentiation and its absence in tumour tissue is associated with an epithelial-to-mesenchymal transition. We further demonstrated that the absence of K17 in skin tumours increases markers of cancer stem-like cells and negatively affects viral protein synthesis.

Conclusions Collectively, our data indicate that K17 expression is a common feature in skin tumorigenesis. While K17 is not primarily targeted by PV oncoproteins, our *in vivo* and *in vitro* data suggest that it is an important regulator of epithelial differentiation and thus may play a role in controlling viral protein synthesis.

Lay summary

The structured formation of various keratins (a type of protein) determines the normal structure of the epidermal skin layers. However, stress keratins are produced only during wound healing, skin diseases and cancer. One of these stress keratins (called K17) is also produced in squamous cell carcinomas (SCCs) of the skin, where UV irradiation and human papillomavirus (HPV) infection are important cofactors. Previous research has reported that K17 is upregulated in papillomavirus (PV)-induced 'benign' (not harmful) skin tumours in mice, and could play a role in promoting tumour growth.

Accepted: 9 June 2024

To investigate whether K17 formation is directly induced by PVs, we analysed levels of K17 in skin tumour samples from different animal models and humans. By looking at K17 levels in the presence of PVs, we were able to show that K17 is not induced by PV proteins. Rather, K17 expression appears to be linked to the differentiation status of the tumour tissue and influences the tumour microenvironment, which means it can play a role in controlling HPV.

Overall, our study findings suggest that K17 expression is a common feature of skin tumours. Although further research is needed, K17 appears to be a reasonable target for the therapy of HPV-related and HPV-unrelated skin SCCs.

What is already known about this topic?

- Cytokeratin 17 (K17) is not expressed in normal tissues, except for stem cell populations in hair follicles.
- Its expression is upregulated in wounded skin and correlates with poor prognosis in several cancers, which suggests that K17 is an important factor in oncogenesis.
- It was previously suggested that K17 expression is induced by a papillomavirus (PV) in a murine animal model to induce an immunological status that is beneficial for tumour growth and viral maintenance.

What does this study add?

- This is the first systematic and comprehensive study analysing K17 expression in skin tumour specimens of different animal models and human skin samples.
- We found that K17 expression is independent of PV oncoproteins, but rather is linked with the differentiation status of the tumour.
- Moreover, in tumours from the *Mastomys coucha* model, we showed that absence of K17 is associated with an epithelial-to-mesenchymal transition of the tissue counteracting viral protein expression.

What is the translational message?

- Our study indicates that K17 expression is a common feature of skin tumorigenesis.
- Indeed, it appears to create an environment with a certain level of differentiation, thereby playing a role in controlling human PV (HPV).
- Although further research is required, K17 may represent a target for therapy of HPV-related and HPV-unrelated squamous cell carcinomas.

The family of keratins comprises 54 proteins. In the skin, the expression patterns of K5/K14 and K1/K10 determine the differentiation status of distinct epidermal layers.[1] However, while the disease-associated keratin 17 (K17) is not expressed in normal tissues except for the stem cell populations in the hair follicles,[2] its expression is rapidly upregulated in wounded skin.[3] Furthermore, K17 expression is correlated with poorer prognosis in breast,[4] pancreatic,[5] colorectal,[6] oropharyngeal[7] and cervical cancers,[8] and K17 is considered to be an important factor in oncogenesis.

K17 is unique among the keratins as it can bind and sequestrate nuclear proteins to the cytoplasm for their degradation and is thereby able to drive cell-cycle progression. Consequently, K17 knockout (K17KO) cells showed lower levels of S- and interphase markers.[3,9]

K17 expression can also be found in cutaneous squamous cell carcinomas (SCCs),[10] a subgroup of nonmelanoma skin cancers. For those cancers, ultraviolet (UV) radiation is a major risk factor. Additionally, certain human papillomaviruses (HPVs), especially HPVs of the genus *Betapapillomavirus* (betaHPVs), are important cofactors, particularly for their premalignant precursor actinic keratosis (AK).[11] Papillomaviruses (PVs) are small nonenveloped double-stranded DNA viruses that infect epithelial keratinocytes.[12] Based on their tissue tropism, they are subdivided into mucosal types, such as HPV16, which can cause anogenital or oropharyngeal cancer[13,14] and cutaneous types associated with SCCs, such as HPV8.[15,16] Several transgenic mouse models have been established to characterize the oncogenic functions of HPV proteins. Mouse models for HPV8 express either the single early genes E2, E6 or E7 or the complete early viral genome region (CER),[17–19] while mouse models for HPV38 and HPV49 express E6 and E7 together.[20,21] HPV16 transgenic mice, originally generated to investigate cervical carcinomas, also develop skin tumours, as the viral oncogenes are also strongly expressed in the skin.[22] These mice express the HPV-transgene under control of the human K14 promoter and therefore cannot mimic the natural course of infection. A very useful animal model in this context is the multimammate African mouse *Mastomys coucha*. These animals are naturally infected with the cutaneous *Mastomys natalensis* papillomavirus (MnPV), the aetiological cause of benign skin tumours.[23] This natural model mimics many aspects of cutaneous HPV infections in humans and allows for the study of the complete infection cycle of a cutaneous PV in its genuine host, starting from infection early in life to the final manifestation of skin tumours.[23,24] Chronically UV-exposed MnPV-infected animals develop cutaneous SCCs significantly more often than virus-free counterparts and during progression,

molecular and phenotypic changes within these tumours lead to a loss of the viral episomes,[25,26] a phenomenon that is also observed in human SCCs.[27] Another animal model that allows for the investigation of a genuine PV are mice infected with *Mus musculus* PV1 (MmuPV1), which infects both cutaneous and mucosal tissues.[28,29]

Although strong K17 expression was reported in skin papillomas of both MmuPV1-infected and transgenic HPV16 mice,[22,30] it is still unclear whether this upregulation is virally induced. Here, we systematically studied K17 expression in skin tumours of HPV8, HPV38 and HPV49 transgenic mice in comparison with spontaneously occurring skin tumours in non-HPV-transgenic animals. We further compared MnPV-positive with MnPV-negative skin tumours of the *Mastomys* model and human HPV-positive with HPV-negative SCCs and AKs.

Materials and methods

Animals and animal tissue specimens

Tissue specimens from *Mastomys coucha* were generated in previous studies.[25,31] The animals were housed and handled in accordance with local (DKFZ), German and European statutes. Experiments were approved by the responsible Animal Ethics Committee for the use and care of live animals (Regional Council of Karlsruhe, Germany, file nos. G26/12 and G289/15). If samples were provided by collaborators, the experiments were conducted in accordance with approval by their respective authorities.

Tissue samples from HPV8 CER, HPV8 E6 and HPV8 E7 mice[17–19] were kindly provided by B. Akgül (University of Cologne). Tissue samples from HPV38 E6/E7 and 4NQO-treated HPV49 E6/E7 and FVB/N wildtype mice[20,21] were kindly provided by D. Viarisio (DKFZ).

Samples of dimethylbenz[a]anthracene (DMBA) and 12-O-tetradecanoyl-phorbol-13-acetate (TPA)-induced skin tumours of C57BL/6 mice[32] were kindly provided by K. Müller-Decker (DKFZ).

Spontaneous mouse papillomas used here as negative controls (Table S1; see Supporting Information) were noticed during regular health checks in the Center for Preclinical Research at the DKFZ, classified by an external pathologist and kindly provided by K. Schmidt (DKFZ).

Human tissue specimens and ethical statement

Clinical specimens were included from a series of tissue samples obtained between September and November 2021 by excision surgery. The study was approved by the Ethical Committee of the University Witten/Herdecke, Germany (reference no. 166/2017). Written patient consent for publication was obtained.

Human sample processing

Human samples (AKs and cutaneous SCCs) were previously analysed for betaHPVs for another study (unpublished). Briefly, the tissue was split for fixation in 4% formalin for tissue analyses and for nucleic acid extraction, respectively. DNA was extracted using the AllPrep DNA/RNA/Protein Mini Kit (Qiagen). DNA was then quantified and subjected to a pan-betaHPV polymerase chain reaction (PCR)[33,34] at the German National Center for Papilloma- and Polyomaviruses (Cologne, Germany) to identify positive samples. DNA from positive samples were further subjected to a reverse hybridization assay (RHA) skin (beta) HPV genotyping test (Labo Bio-medical Products BV, Rijswijk, the Netherlands) that can distinguish between 25 different betaHPV genotypes.[33]

Immunofluorescence staining (tissue)

Staining of formalin-fixed paraffin-embedded (FFPE) tumours was performed as previously described.[25] Briefly, deparaffinized sections were heated in citrate buffer pH6.0 prior to blocking with 5% goat serum in phosphate-buffered saline (PBS). The sections were incubated overnight at 4 °C with antibodies against K17 (W16131A, rat IgG2b, 1 : 1000, BioLegend, San Diego, CA, USA), CD271 (rabbit IgG, #8238, 1 : 250, Cell Signaling Technology, Danvers, MA, USA), E-cadherin (610181, mouse IgG2a, 1 : 500, BD Biosciences, Franklin Lakes, NJ, USA), vimentin (#5741, rabbit IgG, 1 : 100, Cell Signaling Technology) or HPV8 E4 (8E4, rabbit IgG, 1:200, kindly provided by J. Doorbar) diluted in 1% goat serum in PBS. MnPV-E4 was detected with anti-mouse-IgG2b-Alexa594 (A21145, 1 : 2000, Invitrogen, Waltham, MA, USA), HPV8 E4 with antirabbit-IgG-Alexa594 (A11072, 1 : 2000, Invitrogen), K17 with antirat-IgG2b-Alexa488 (MRG2b-85, 1 : 300, BioLegend), E-cadherin with antimouse IgG2a Alexa488 (A21131, 1 : 2000, Invitrogen), vimentin with antirabbit-IgG-Alexa488 (Invitrogen, A11008, 1 : 2000) and nuclei were stained with 4′,6-diamidino-2-phenylindole (DAPI). Sections were mounted with Dako Faramount Aqueous Mounting Medium (Dako, Santa Clara, CA, USA).

Preparation of nucleic acids from murine tissue

Fresh tissue samples were frozen in TE buffer and homogenized using Precellys tubes with ceramic beads and a Precellys 24 homogenizer. DNA was extracted using chloroform:isoamyl alcohol, as described elsewhere.[35]

Sections of FFPE mouse tissue (total thickness of 120–600 μm, depending on the size of the sample) were cut into reaction tubes and processed as previously described.[36] Briefly, tissue sections were deparaffinized for 10 min at 95 °C in lysis buffer (0.5% Tween20, 1 mmol L^{-1} ethylenediaminetetraacetic acid, 50 mmol L^{-1} Tris-HCl pH8.5) prior to a second incubation for 10 min at 65 °C in fresh lysis buffer. The tissue was scratched from the glass using a 23G cannula and subjected in 12 μL lysis buffer incl. 20 μg mL^{-1} proteinase K. After overnight digestion at 65 °C, the sample was spun down and the enzyme was inactivated for 10 min at 95 °C. The sample was chilled on ice and spun down prior to addition of 4 μl H_2O. 4 μL of this mix were used per subsequent MmuPV1 detection PCR.

Detection of *Mus musculus* papilloma virus 1 via polymerase chain reaction

PCR amplification of MmuPV1 DNA (primers: 5′-GCACCCTC-CGTGTACTTTGG-3′, 5′-CAG CGAGTTGCCGATGATGT-3′) and glyceraldehyde 3-phosphate dehydrogenase (primers: 5′-CTTCATTGACCTCAACTACATGGTC-3′, 5′-GCAGT-GATGGCATGGACTGTG-3′) from FFPE mouse tissue was

performed using Platinum Taq DNA Polymerase. Thermal cycling conditions for PCRs were based on a primary denaturation step at 94 °C for 3 min, followed by 40 cycles of 30 s at 94 °C, 30 s at 60 °C, 20 s at 72 °C and a final extension step of 5 min at 72 °C. DNA fragments were separated by agarose gel electrophoresis, stained with ethidium bromide and visualized using UV radiation.

Quantitative polymerase chain reaction for Mastomys natalensis papillomavirus DNA load

Quantification of MnPV DNA was performed using the iTaq Universal SYBR Green Supermix (Bio-Rad, Hercules, CA, USA) as previously described.[25] Briefly, 2 μL DNA (approximately 10 ng) per reaction were mixed with 0.5 μmol L^{-1} forward/reverse primers for MnPV *L1* (5′-ACGGCAACTCATGCTTCTTC-3′, 5′-CTCTGTGCCTGTCCATCCTT-3′) or the single-copy-number gene β-Globin to determine the number of input cell equivalents (*Mastomys coucha*: 5′-ACCATGGTGCACCTTACTGAC-3′, 5′-TCCAGGCACCCAACTTCTAC-3′). MnPV copy numbers were determined in duplicates and defined as the number of MnPV genomes per two β-globin copies. In order to categorize a sample measured in this study as positive or negative, we used the cutoff value of 0.346 copies per cell determined in a previous study.[24]

Cell culture conditions

HeLa and HeLa K17KD cells were grown in Dulbecco's Modified Eagle Medium (DMEM) supplemented with 5% fetal calf serum (FCS). HeLaT cells were grown in DMEM supplemented with 10% FCS. For all cell lines, media were supplemented with 1% penicillin/streptomycin and 1% L-glutamine. Media of HeLaT and 293TT cells were further supplemented with hygromycin B (125 μg mL^{-1}) to maintain additional SV40 large T-antigen expression. Primary human keratinocytes (PHKs) were obtained from Lonza Biosciences (catalogue no. 00192907, lot no. 0000188311, Lonza, Cologne, Germany). PHKs and N/TERTs[37] were grown in keratinocyte growth medium 2 (#C-20011, PromoCell, Heidelberg, Germany) with 1% penicillin/streptomycin (PS, #15140130, Thermo Fisher Scientific, Waltham, MA, USA). All cell lines were kept at 37 °C, 5% CO_2 and 95% humidity and regularly checked for mycoplasma via PCR.

Generation of sgRNAs for K17 knockout

For CRISPR/Cas9-mediated genome editing of *Krt17*, intended to be a knockout but actually being a knockdown on protein level, individual single guide RNAs (sgRNAs; HeLa K17KO1: 5′-CACGCATCTCGTTGAGGATG-3′; HeLa K17KO2: 5′-ACAGATTGACAATGCCCGTC-3′) were designed using the web tool CHOPCHOP[38] and subcloned into pLentiCRISPRv2 as previously described.[39] After lentiviral infection, selection and gDNA isolation, the regions around the cleavage sites were amplified by PCR using KO-specific primers (HeLa K17KO1: 5′-TGAGATCAATGTGGAGATGGAC-3′ and 5′-GGGCTTACTGTCAGTGCTAAGG-3′; HeLa K17KO2: 5′-CCAATGACCTGACTACTCTCCC-3′ and 5′-CTTCACTGCATCCTGGACTAAG-3′). Successful sgRNA integration was validated by Sanger sequencing of the amplicons using a human U6-specific primer (5′-ACTATCATATGCTTACCGTAAC-3′). Effective site-specific cleavage of DNA strands was validated using the T7 endonuclease assay as previously described.[40] Additionally, the indel (insertion/deletion) frequency of the individual sgRNAs was predicted by subjecting the sequencing data to the Inference of CRISPR Edits (ICE) software tool from Synthego (Redwood City, CA, USA).[41]

Retroviral transduction

The production of retroviruses and the retroviral transduction of human cells with recombinant retroviruses coding for HPV was carried out as previously described.[25,42] Briefly, retro/lentiviral supernatants were mixed with 5 μg mL^{-1} hexadimethrine bromide (polybrene) and added to the cells. At 2 days postinfection, cells were selected by adding 500 μg mL^{-1} G418. The generation of pLXSN-based retroviral vectors coding for HPV8 E6, E7 or E6/E7 and the confirmation of early gene expression by reverse transcription (RT)-qPCR have been previously described.[43–45]

K17 immunofluorescence staining (cells)

HeLa K17KD cells were grown on glass cover slides for 48 h prior to washing with PBS and fixing for 10 min in 4% paraformaldehyde. Cells were blocked in 10% goat serum/0.3% Triton X-100 in PBS for 1 h and stained overnight at 4 °C with anti-K17 (W16131A, rat IgG2b, 1 : 1000, BioLegend) prior to washing and incubation for 45 min at room temperature with antirat-IgG2b-Alexa488 (MRG2b-85, 1 : 300, BioLegend). Nuclei were stained with DAPI. Cover slides were mounted with Faramount Aqueous Mounting Medium (Dako) and imaged with a Cell Observer.Z1 (Carl Zeiss, Oberkochen, Germany).

Check of *KRT17* expression

RT-qPCR for check of expression of *KRT17* (primers: 0.125 μmol L^{-1}; 5′-CATGCAGGCCTTGGAGATAGA-3′, 5′-CACGCAGTAGCGGTTCTCTGT-3′) and HPV18 E6/E7 (primers: 0.1 μmol L^{-1}; 5′-ATGCATGGACCTAAGGCAAC-3′, 5′-AGGTCGTCTGCTGAGCTTTC-3′) was performed using the iTaq Universal SYBR Green Supermix (Bio-Rad, Hercules, CA, USA) with 10 ng cDNA per reaction mixed with primers. The reference gene *HPRT1* (primers: 0.125 μmol L^{-1}; 5′-GAAGGAGATGGGAGGCCATC-3′, 5′-CTTTTATGTCCCCCGTTGACTG-3′) was used for normalization.

Western blotting

Cells were lysed on ice for 30 min in radioimmunoprecipitation assay (RIPA) buffer, heated for 5 min at 95 °C, chilled on ice and spun down. Protein concentrations were measured via Bradford Assay. For each sample, 30–100 μg were mixed with loading dye, heated for 5 min 95 °C, briefly chilled on ice and loaded onto 12% gels for sodium dodecyl sulfate–polyacrylamide gel electrophoresis. After blotting, proteins were detected with antibodies against vinculin (sc-73614, 1 : 4000, Santa Cruz, Dallas, TX, USA), c-Myc (ab32072; 1 : 1000, Abcam, Cambridge, UK), K17 (W16131A, 1 : 500, BioLegend), tubulin (sc-63029, 1 : 4000, Santa Cruz), proliferating cell nuclear antigen (PCNA) (#13110; 1 :

2000, Cell Signaling Technology), CD271 (#8238; 1 : 2000, Cell Signaling Technology), CD44 (#37259; 1 : 1500, Cell Signaling Technology), active β-catenin (#19807, 1 : 1000, Cell Signaling Technology) or HPV18 E7 (kind gift from Karin Hoppe-Seyler, DKFZ). Detection was achieved with goat antimouse-horseradish peroxidase (HRP) (W4021, 1 : 10 000, Promega, Madison, WI, USA), antirabbit-HRP (W4011, 1 : 10 000, Promega, Madison, WI, USA), goat antirat-HRP (1 : 10 000, Jackson ImmunoResearch, West Grove, PA, USA) or IRDye-coupled goat antirat-680RD (926-68076, 1 : 4000, LI-COR, Lincoln, NE, USA). For the latter, signals were detected using a LI-COR Odyssey Fc imager (LI-COR).

Virus-like particle enzyme-linked immunosorbent assay

Virus-like particle (VLP) enzyme-linked immunosorbent assays (ELISAs) were performed as previously described.[46] Briefly, 96-well ELISA plates (Nunc PolySorp, Thermo Fisher Scientific) were coated with 100 ng per well purified high-quality $L1_{SHORT}$-VLPs in 50 mmol L^{-1} carbonate buffer pH9.6. The next day, plates were blocked with casein blocking buffer (CBB) and incubated for 1 h with threefold dilutions of *Mastomys* sera in CBB. Then, plates were washed four times using PBS with Tween (PBST) and incubated with goat antimouse IgG-HRP (1 : 10 000 in CBB). After four washes, colour development and measurement were performed as described for the glutathione S-transferase ELISA. Antibody titre represents the last reciprocal serum dilution above the blank.

E2 enzyme-linked immunosorbent assay

The ELISA was performed as recently described.[47] Briefly, 96-well ELISA plates (Nunc PolySorp) were coated overnight at 4 °C with glutathione-casein diluted in carbonate buffer (pH9.6). The next day, the plate was blocked for 1 h at 37 °C with CBB (CBB, 0.2% casein in PBST: 0.05% Tween-20 in PBS) and then incubated with the respective antigen (bacterial lysate containing GST-antigen-SV40-tag fusion protein) for 1 h. To remove unspecific reaction against bacterial proteins or the GST-SV40-tag fusion protein, *Mastomys* sera were diluted 1 : 50 in CBB containing GST-SV40-tag and preincubated for 1 h. ELISA plates were washed four times with PBST and preincubated sera was added. After 1 h, plates were washed four times and HRP-conjugated goat antimouse IgG (H + L) antibody (1 : 10 000 in CBB, Promega) was applied for 1 h. Antibodies were quantified colorimetrically by incubating with 100 µL per well substrate buffer for 8 min (0.1 mg mL^{-1} tetramethylbenzidine and 0.006% H_2O_2 in 100 mmol L^{-1} sodium acetate, pH6.0). The enzymatic reaction was stopped with 50 µL per well 1 mol L^{-1} sulfuric acid. The absorption was measured at 450 nm in a microplate reader (Labsystems Multiskan, Thermo Fisher Scientific). To calculate the serum reactivity against the respective antigen, sera were tested in parallel against the GST-SV40-tag fusion protein and the reactivity was subtracted from the reactivity against the GST-antigen-SV40-tag. Each ELISA was performed in duplicates at least. The cutoffs were calculated individually for each antigen by measuring sera of virus-free animals.

Pseudovirion-based infection assay

Pseudovirions of HPV18[47,48] (kind gift from Martin Müller, DKFZ) were serially diluted 1 : 3 in 96-well cell culture plates (Greiner Bio-One GmbH, Kremsmünster, Austria) using a suspension of 4×10^4 cells per mL of HeLa cells starting from a 1 : 300 pseudovirion dilution. The resulting 100 µL per well contained 5000 cells per well and diluted pseudovirions and were cultured for 48 h at 37 °C. The activity of secreted Gaussia luciferase was measured 15 min after adding coelenterazine substrate and Gaussia glow juice (PJK Biotech, Kleinblittersdorf, Germany) according to the manufacturer's instructions in a microplate luminescence reader (Synergy 2, BioTek, Thermo Fisher Scientific).

Results

K17 is induced in skin tumours of human papillomavirus transgenic mouse models

We first subjected skin tumours from five transgenic mouse models for cutaneous HPVs to K17 staining. In papillomas and SCCs of HPV8 CER mice, strong K17 staining was observed throughout the complete lesion, which was also stained positive for the viral E4 protein, confirming transgene expression (Figure 1a). The same observation could be made in SCCs of HPV8 E6 mice (Figure 1b), while skin tumours of HPV8 E7 mice only showed weak K17 levels, mainly around hair follicles (Figure 1c). In skin SCCs of HPV38 E6/E7 mice (Figure 1d) and in oesophageal tumours of HPV49 E6/E7 mice, elevated levels of K17 could be discerned (Figure 1e). K17 detection in epithelial tumours of these HPV-transgenic mice, is therefore in line with previous observations in skin papillomas of HPV16 E7 mice.[22]

K17 is also upregulated in murine papillomas without papillomavirus context

To determine whether changes in protein levels in virus-induced tumours are linked to the expression of the viral oncogene and not to the tumorigenic process as such, the experiments required the inclusion of matched control tissue. With regard to K17, normal skin is not a suitable control tissue, as K17 becomes upregulated only after wounding or mitogenic stimuli.[2] To overcome this limitation, we acquired seven skin tumour samples from transgenic mice with non-HPV backgrounds that were previously noticed during regular health checks in our animal facility (for further information, please refer to Table S1). As expected, staining of nonlesional normal murine skin detected K17 only in hair follicles (Figure 2a). In order to exclude unpredicted MmuPV1 infections in these mice, DNA was extracted from fresh-frozen skin, tumour tissue (Figure 2b) or FFPE material (Figure 2c) of the samples shown in Figure 2d–h or from additional animals of the respective mouse colonies. MmuPV1 DNA could not be detected in any of the samples tested, while positive PCRs for glyceraldehyde 3-phosphate dehydrogenase confirmed successful DNA extraction. Contrary to normal skin (Figure 2a), strong K17 expression could be detected in all PV-unrelated papillomas, and well-differentiated lesions

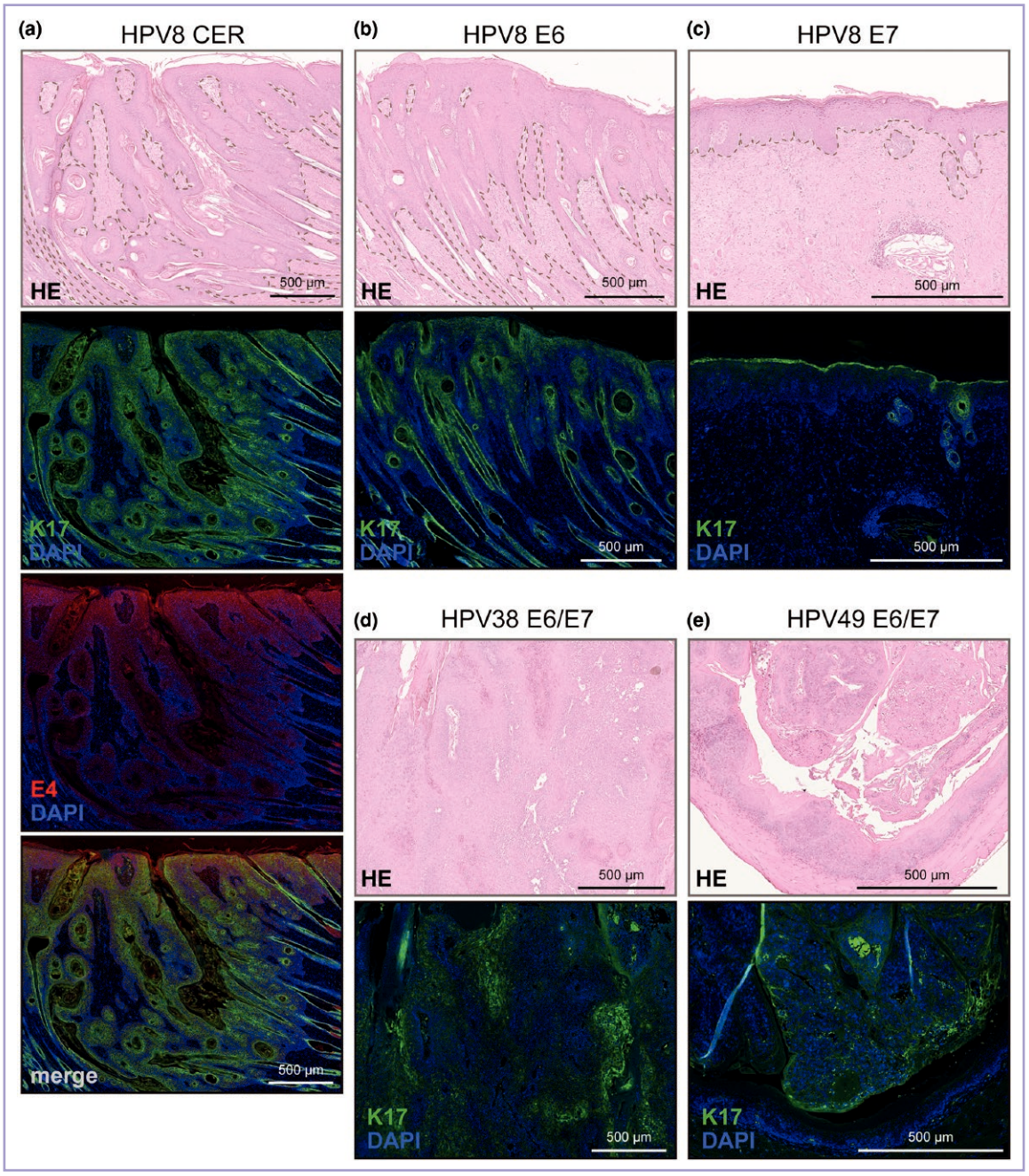

Figure 1 K17 expression in skin tumours from transgenic human papillomavirus (HPV) mouse models. Elevated K17 (green) levels in skin papillomas of (a) HPV8 complete early viral genome region (CER) mice expressing the complete early region [E4 (red)] and (b) HPV8 E6 mice, but not in (c) HPV8 E7 mice. K17 (green) is also detectable in (d) squamous cell carcinomas (SCCs) of chronically ultraviolet-irradiated HPV38 E6/E7 mice and (e) oesophageal tumours in HPV49 E6/E7 mice induced by 4-nitroquinoline 1-oxide (4NQO). Nuclei were stained with 4′,6-diamidino-2-phenylindole (DAPI) (blue). HE, haematoxylin and eosin.

were classified as exophytic epithelial hyperplasia with orthokeratosis, independent of their genetic background (Figure 2d–f). Moreover, K17 was detected in 4NQO-induced oesophageal tumours of FVB/N wildtype mice (two of two samples) (Figure 2d) and in skin tumours induced with dimethylbenz[a]anthracene (DMBA) and 12-O-tetradecanoyl-phorbol-13-acetate (TPA) in C57BL/6 wildtype mice (three of three samples) (Figure 2e). These results indicate that epithelial tumorigenesis in mice is associated with K17 overexpression, independent of the presence of the HPV oncoproteins.

K17 expression in skin tumours of *Mastomys coucha*

Animals from the MnPV-infected and MnPV-free *Mastomys coucha* colonies were next used to examine K17 expression in the context of cutaneous PV infection. Ongoing MnPV infections in these animals can be revealed by qPCR and tissue staining with a MnPV E4-specific antibody, while E2- and VLP-ELISAs confirm preceding infections.[47] As in mice, K17 expression is low in nonlesional skin except in the hair follicles, but is strongly induced in proliferating

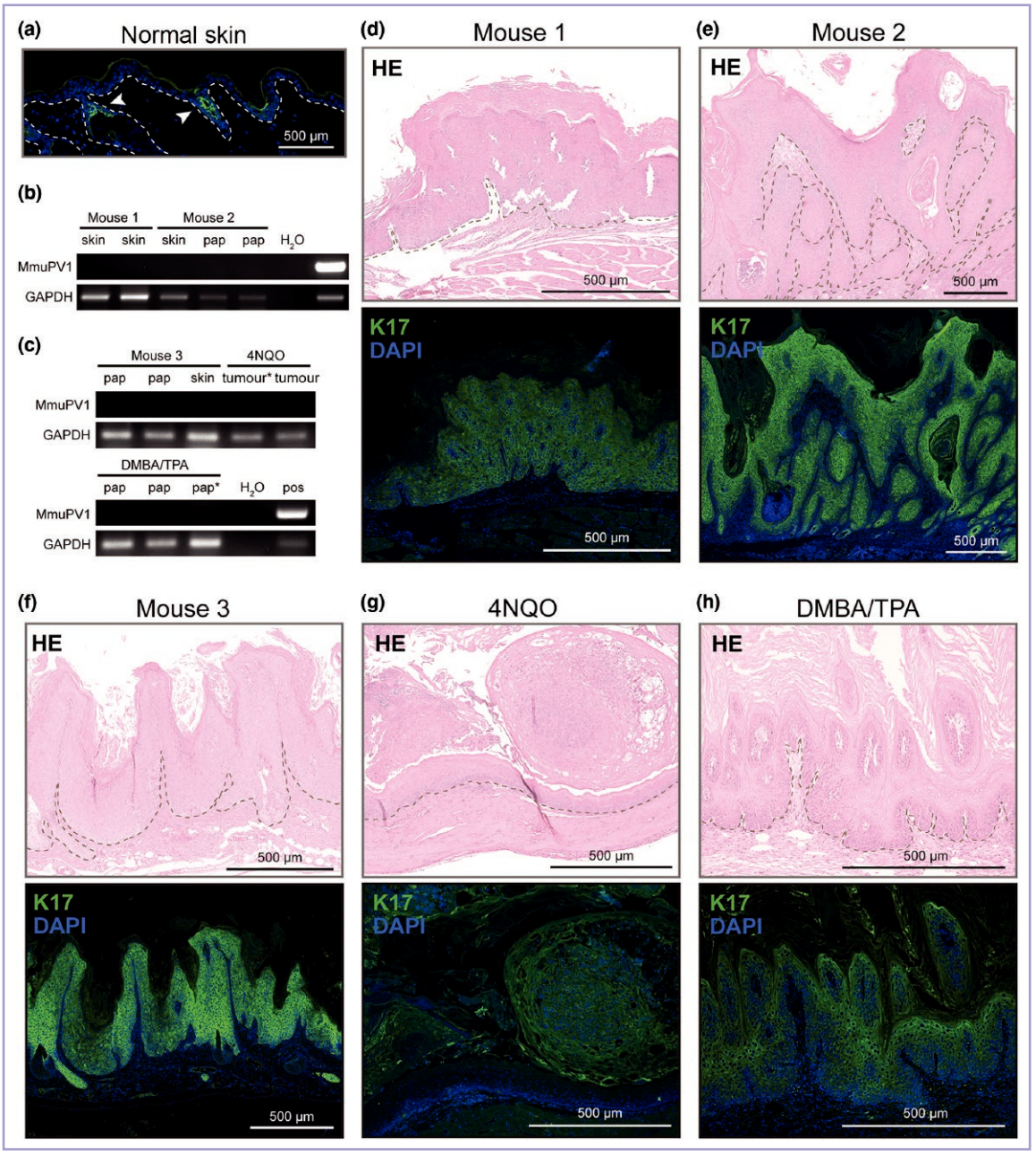

Figure 2 Elevated K17 expression in papillomavirus (PV)-negative skin tumours from mice. K17 (green) can only be detected in hair follicles of normal skin (indicated by white arrows), while the epidermis is negative. Nuclei were stained with DAPI (blue). (b) Verification of MmuPV1-negativity of non-human PV (HPV) transgenic mice 1 (panel d) and 2 (panel e) using fresh tissue from additional animals of the same colony. (c) Verification of MmuPV1-negativity in the tumours and colonies of transgenic mouse 3 (panel f), FVB/N mice (panel g) and C57BL/6 mice (panel h) using formalin-fixed paraffin-embedded tissue (* indicates samples of which a K17 staining is shown, remaining samples derived from additional animals of the same colony). (d–f) Spontaneous skin papillomas of non-HPV-transgenic mice, (g) a 4NQO-induced oesophageal tumour of an FVB/N wildtype mouse, (h) a DMBA/TPA-induced papilloma of a C57BL/6 wildtype mouse. DAPI, 4′,6-diamidino-2-phenylindole; DMBA, dimethylbenz[a]anthracene; GAPDH, glyceraldehyde 3-phosphate dehydrogenase; HE, haematoxylin and eosin; NQO, nitroquinoline-1-oxide TPA, tetradecanoylphorbol-13-acetate.

keratinocytes during wound healing (Figure 3). Tissue staining showed strong K17 expression in MnPV-induced benign skin tumours (papillomas and keratoacanthomas), which correlated with strong MnPV E4 staining, a high viral load in the tumour tissue and seroconversion against MnPV E2 or viral capsids as measured by ELISA (Figure 4a).

Chronically UV-irradiated MnPV-infected *Mastomys* develop cutaneous SCCs significantly more often than virus-free UV-irradiated animals.[25] These SCCs can be divided into well-differentiated keratinizing SCCs (KSCCs) with high viral loads and poorly differentiated nonkeratinizing SCCs (nKSCCs) with low viral loads (Figure 4b, c).[25] While KSCCs also showed moderate-to-strong K17 staining and active viral infection (shown as MnPV E4 expression) throughout all squamous layers (Figure 4b), nKSCCs were unevenly stained for K17 (Figure 3c). In nKSCCs, K17 could be found in the differentiated areas (Figure 4c, indicated by the asterisk) that were also positive for the epithelial marker E-cadherin

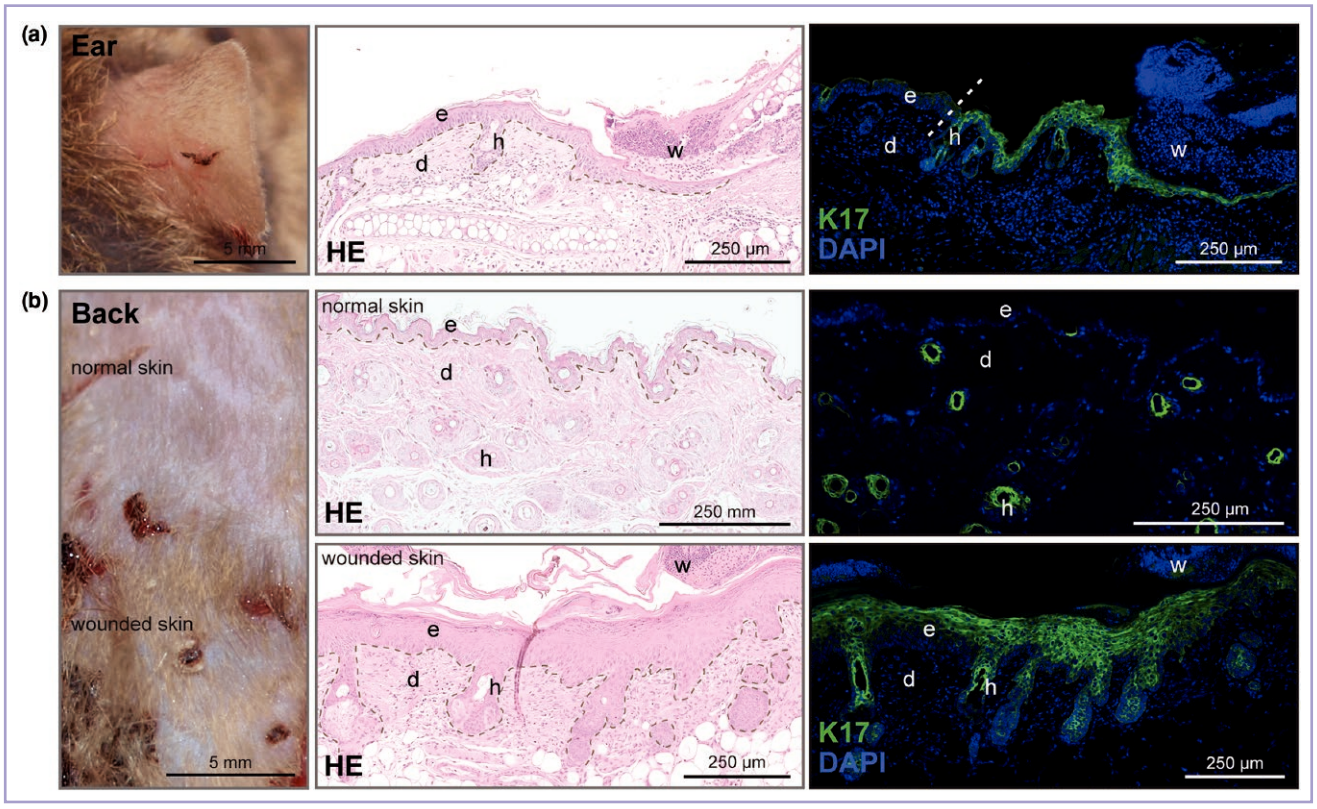

Figure 3 Elevated K17 levels during skin wound healing in *Mastomys coucha*. (a) Staining of a superficial ear wound. Hyperproliferating keratinocytes showed increased K17 (green) expression. Apart from the wound, K17 levels were low (compare the left and right parts of the immunofluorescence staining). (b) Representative stainings of normal skin and skin wounds of the back that show epidermal K17 upregulation. d, dermis; e, epidermis; h, hair follicle; w, wound/ulceration; DAPI, 4′,6-diamidino-2-phenylindole; HE, haematoxylin and eosin.

(Figure S1; see Supporting Information). In contrast, K17 was not expressed in nondifferentiated lower layers (Figure 4c, indicated by #) that were positive for vimentin (Figure S1). The switch of E-cadherin to vimentin expression is considered an indicator for an epithelial-to-mesenchymal transition (EMT) in the skin.[49] In line with these results, recently performed spatial proteomics of different skin tumour entities of *Mastomys coucha*[26] revealed higher levels of stress keratins in differentiated areas when compared with dedifferentiated areas of nKSCCs (Table S2; see Supporting Information). Furthermore, bioinformatical analyses of these proteome data indicated regulatory networks related to an EMT, which can lead to an increase of cancer stem-like cells (CSCs)[50] that are characterized by coexpression of CD44 (a major hyaluronan receptor) and CD271 [nerve growth factor (NGF) receptor].[51,52] Notably, correlating with an absence of both K17 and E-cadherin and increased vimentin levels (Figures S1 and S3), we also found CD44 significantly enriched in dedifferentiated areas of SCCs when compared with normal epidermis [log2 fold change (FC) = 0.96, P_{adj} = 0.036]. In contrast, compared with normal skin, CD44 was not altered in well-differentiated SCC areas (log2 FC = 0.55, P_{adj} = 0.72), but was decreased in MnPV-induced benign tumours (log2 FC = -0.79, P_{adj} = 0.038).[26] Interestingly, bioinformatical analyses predicted upregulated NGF signalling in dedifferentiated SCC areas, which can foster stem-like properties and tumorigenicity[53] and is linked to tumour growth and metastasis.[54] Strikingly, in line with these previous results, CD271 levels increase when tumour cells dedifferentiate (Figure S2; see Supporting Information).[26] Taken together, these data clearly point to a differentiation-dependent regulation of K17 in skin tumours and a switch to a dedifferentiated epithelial state that may counteract viral maintenance.

Skin tumours in *Mastomys coucha* not induced by *Mastomys natalensis* papillomavirus are also K17 positive

As in mice, *Mastomys coucha* usually do not develop spontaneous skin lesions without infection with MnPV[35] or by carcinogenic DMBA/TPA treatment.[55] However, we coincidentally found a strongly keratinized ear tumour of an untreated *Mastomys coucha* that was never infected by MnPV as clearly shown by qPCR of the tumour tissue and serological analyses (Figure 5a). This spontaneously developed keratoacanthoma also showed high K17 levels. In a previous study focusing on the interplay between MnPV infection and UV radiation, two MnPV-free UV-irradiated control animals developed SCCs, which were histologically classified as KSCC (Figure 5b) and nKSCC (Figure 5c), respectively. Despite the lack of MnPV, both tumour entities showed elevated K17 levels, which were again correlated with the differentiation status of the respective areas in nKSCCs (Figure 5b, c), as demonstrated again by E-cadherin and vimentin costaining (Figure S3; see Supporting Information).

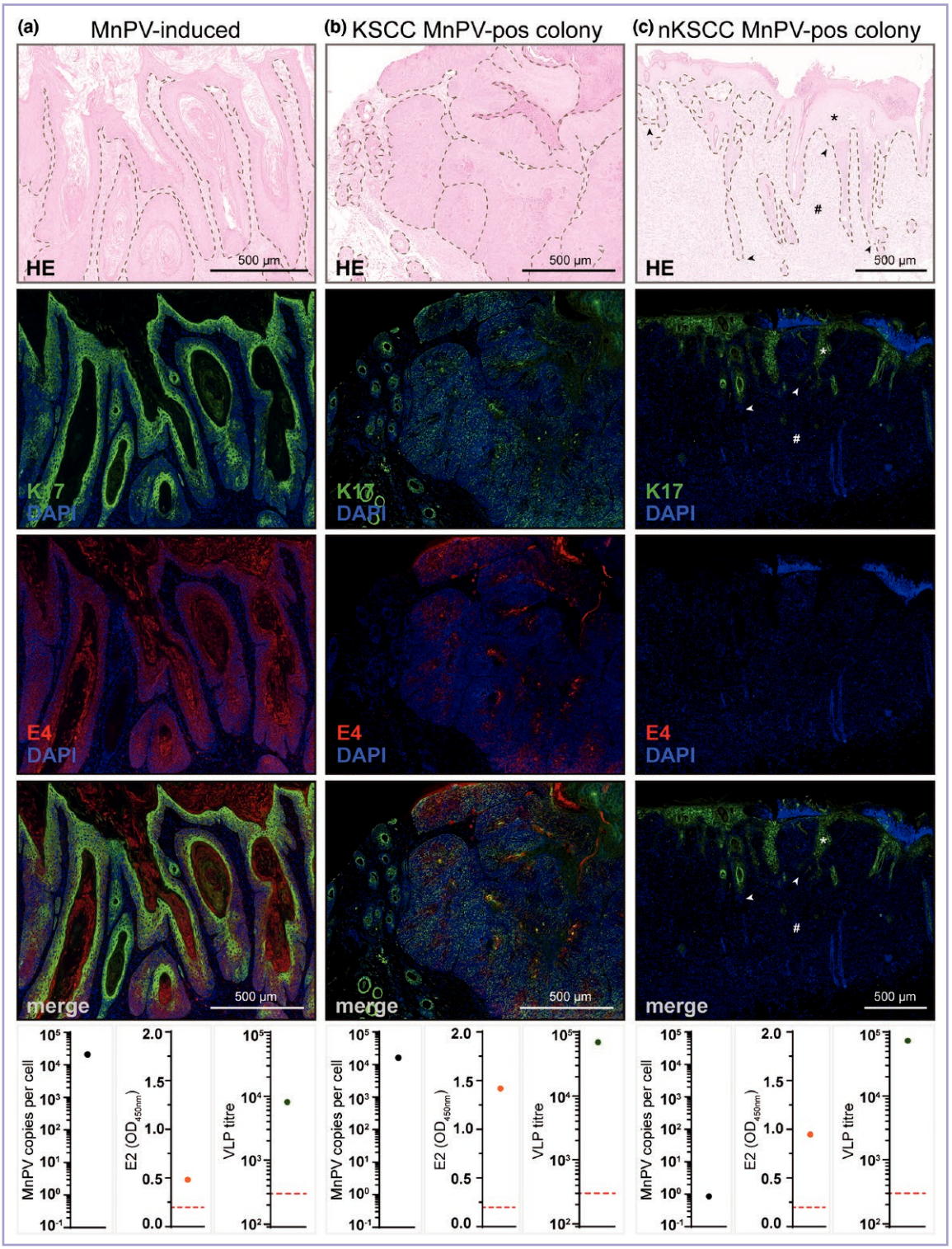

Figure 4 K17 expression in skin tumours of the natural infection model *Mastomys coucha*. Elevated K17 (green) levels were detectable in all epithelial layers of (a) benign *Mastomys natalensis* papillomavirus (MnPV)-induced skin papillomas and (b) well-differentiated squamous cell carcinomas (SCCs) induced by MnPV infection and chronic ultraviolet irradiation. Active MnPV infection was visualized by E4 staining (red). (c) In dedifferentiating SCCs with low viral loads, K17 expression in well-differentiated areas (*) is lost during phenotypic changes from altered keratinocytes to spindle cells (#). Arrows indicate transition zones. Nuclei were stained with DAPI (blue). MnPV DNA loads in the respective lesions were detected via quantitative polymerase chain reaction and preceding infections of the animals were further indicated by seroconversion against viral antigens measured using Glutathione S-transferase E2 enzyme-linked immunosorbent assay (ELISA) and virus-like particle (VLP) ELISA. Dashed red lines indicate the cutoff of the respective method. DAPI, 4′,6-diamidino-2-phenylindole; HE, haematoxylin and eosin; pos, positive.

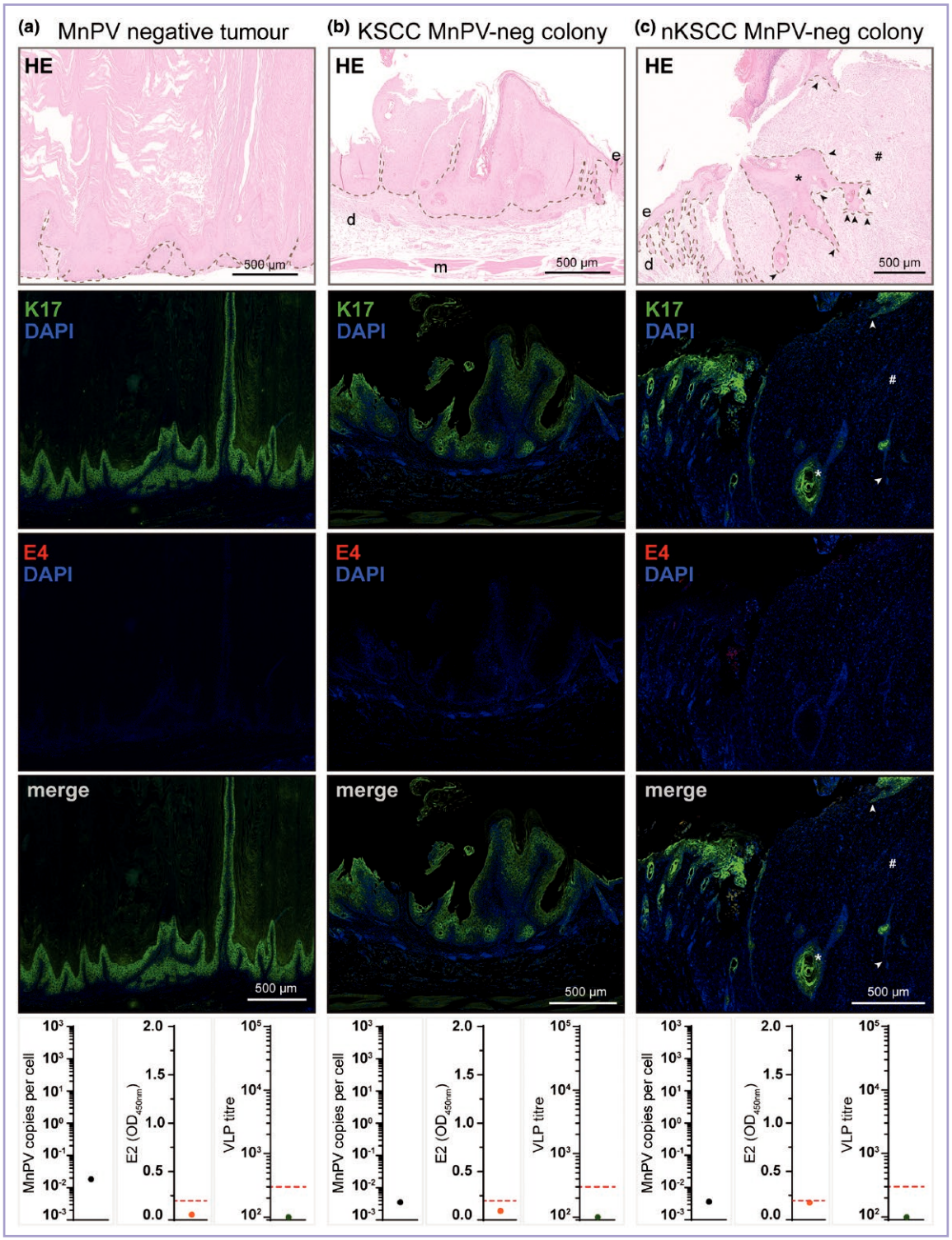

Figure 5 K17 is expressed in *Mastomys coucha* skin tumours not induced by *Mastomys natalensis* papillomavirus (MnPV). (a) Strong K17 (green) expression in all epithelial layers of a spontaneous benign keratoacanthoma on the ear of a *Mastomys*. Nuclei were stained with DAPI (blue). Although originating from the MnPV-positive colony, no active MnPV infection was detected by MnPV E4 staining (red) and quantitative polymerase chain reaction. Glutathione S-transferase E2 and virus-like particle (VLP) enzyme-linked immunosorbent assay further excluded preceding infections of the animal. Red dashed lines indicate the cutoffs of the respective method. (b) K17 is also strongly expressed in well-differentiated keratinizing squamous cell carcinomas (SCCs) from *Mastomys* of the MnPV-free colony induced by chronic ultraviolet (UV)-irradiation. (c) In poorly differentiated nonkeratinizing UV-induced SCCs on MnPV-free animals, K17 expression was detectable in well-differentiated areas (*), but lost in altered keratinocytes with a spindle cell phenotype (#). Arrows indicate transition zones. d, dermis; e, epidermis; m, muscle. DAPI, 4′,6-diamidino-2-phenylindole; HE, haematoxylin and eosin; neg, negative.

Comparison of K17 levels in human papillomavirus-positive and human papillomavirus-negative human skin cancer

As there may be inherent limitations when transferring results from animal models to humans, we investigated K17 in human skin lesions obtained from excisional surgery. The HPV infection status was determined via pan-betaHPV PCR. In case of a positive result, the individual betaHPV types were subsequently identified via reverse hybridization assay.[33,34] In line with the rodent models, strong K17 expression was found in the dysplastic epidermis of HPV-positive AKs (one of one) (Figure 6a) and SCCs (one of one) (Figure 6b), irrespective of the individual betaHPV-type profile identified in these specimens. Importantly, strong K17 expression was also found in HPV-negative AKs (two of two) (Figure 6c) and SCCs (two of two) (Figure 6d). The fact that K17 was found in human premalignant AKs and SCCs even in the absence of detectable betaHPVs provides further confirmation that K17 expression occurs in skin tumours independently of the presence of HPV.

K17 expression affects proteins required for papillomavirus maintenance

To mechanistically support our *in vivo* results, we aimed to analyse the effects of K17 loss in cell culture in the context of PV infection. Keratinocytes in cell culture generally express K17 irrespective of whether they express HPV oncogenes (Figure 7a), indicating that K17 expression is

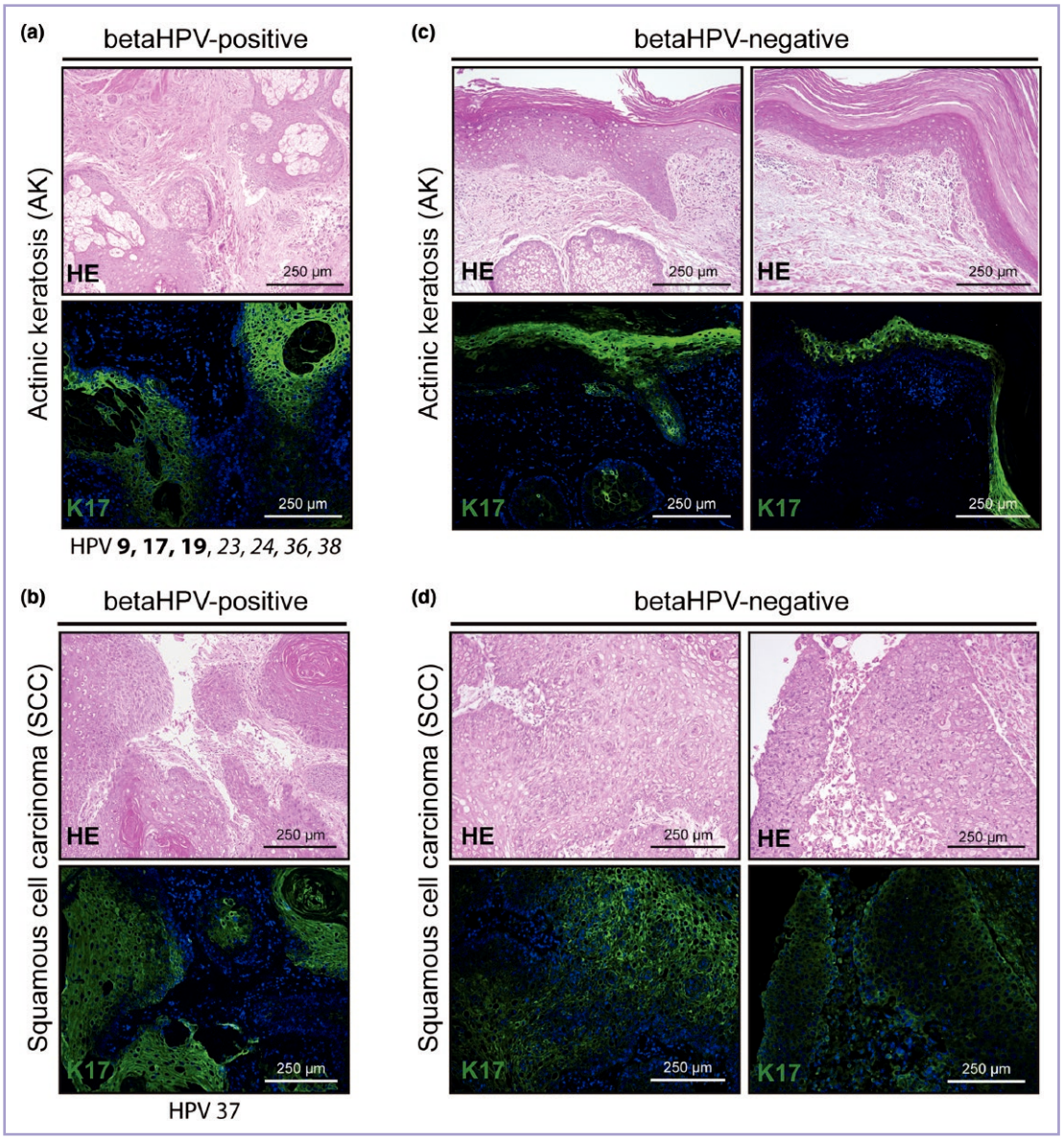

Figure 6 K17 expression in human skin lesions occurs independently of beta human papillomavirus (HPV) presence. Elevated K17 levels can be found in dysplastic epidermis of (a) HPV-positive actinic keratoses (AKs) (b) squamous cell carcinomas (SCCs) and in (c) HPV-negative AKs and (d) SCCs. Nuclei were stained with DAPI (blue). HPV-positivity was determined via polymerase chain reaction and pan-betaHPV-specific primers. Positive samples were subsequently HPV-typed via betaHPV line blot. The betaHPV types identified are indicated below the staining. Bold indicates strong signals; italic indicates weak signals. DAPI, 4′,6-diamidino-2-phenylindole; HE, haematoxylin and eosin.

linked to keratinocyte proliferation *in vitro*. Previous studies focusing on K17 were performed in cervical cancer cells[9] or HeLa cells,[3] in which this keratin was knocked out without considering that these cells contain transcriptionally active integrated HPV18 genomes. Accordingly, the effect of K17 loss on viral oncogene expression has not been investigated. Although this cell line and HPV18 are not the optimal model to study cutaneous HPV biology, for the sake of comparability to previous results we also used HeLa cells to generate two HeLa K17 KO cell lines, which indeed turned out to only have a K17 knockdown (K17KD1 and K17KD2). Using CRISPR/Cas9 genome editing, indels were inserted at different sites of the *KRT17* gene, leading to a substantial reduction in *KRT17* mRNA in cell line K17KD2 (Figure 7b, c). While the increased *KRT17* mRNA levels in K17KD1 suggest an autoregulatory feedback loop aiming to increase *KRT17* expression after loss of the protein, the significantly diminished *KRT17* mRNA levels in K17KD2 indicate a nonsense-mediated mRNA decay.[56] Notably, two additional edited cell lines with even better values regarding knockout quality check could not be cultured over a longer time, also indicating the need for at least some KRT17 expression for successful cell propagation *in vitro* (data not shown).

More importantly, both K17KD cell lines showed a substantial loss of K17 when compared with control cells (Figure 7d, e). In line with previous studies,[3] we observed decelerated proliferation in both K17KD1 and K17KD2 lines as indicated by decreased levels of the proliferation marker

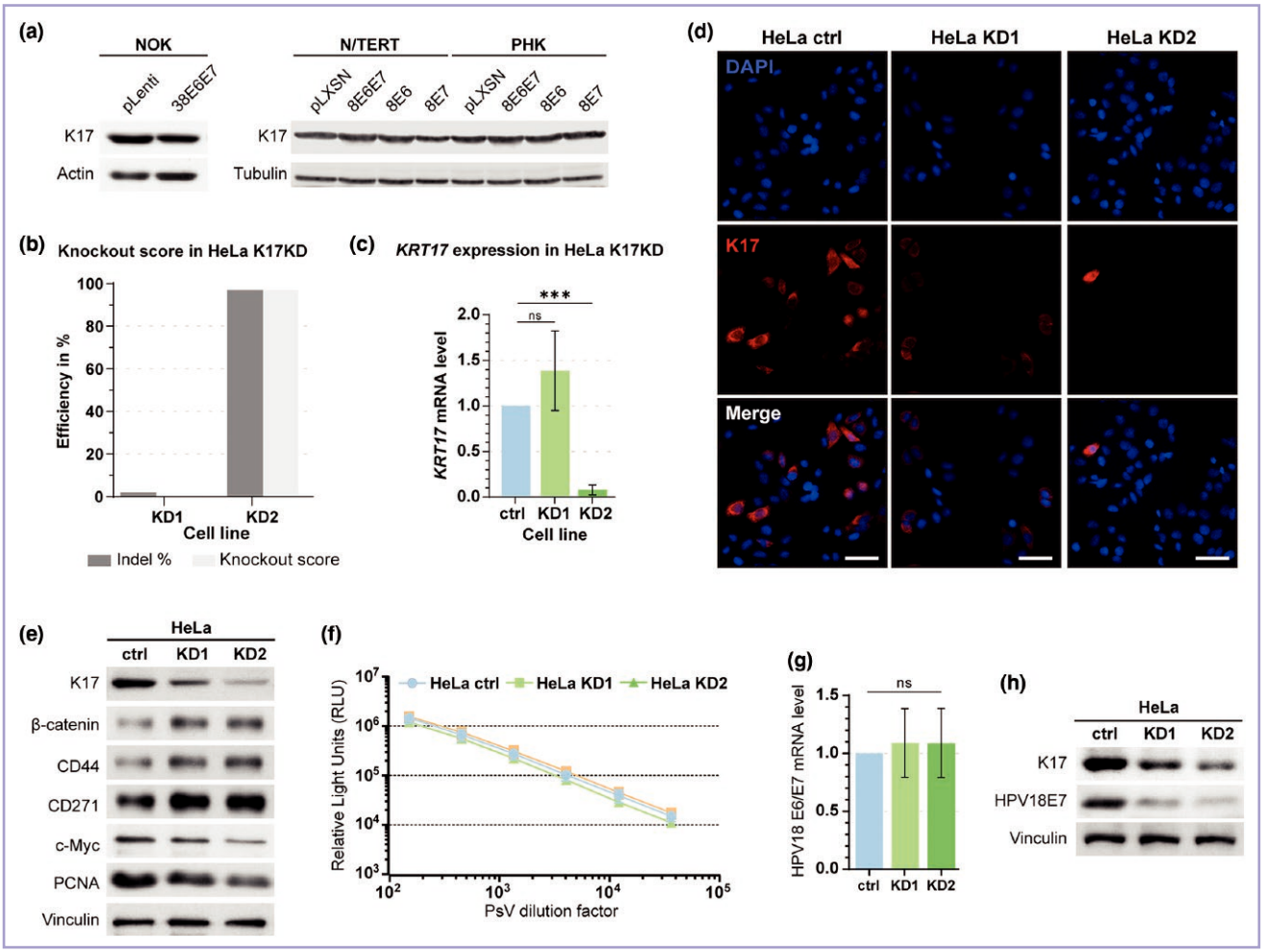

Figure 7 Loss of K17 affects cellular regulators and viral oncoprotein synthesis in HeLa cells. (a) Western blotting showed nearly equal K17 levels in cells stably expressing papillomavirus (PV) oncoproteins compared with the respective control cell line. Human normal oral keratinocytes (NOKs) were transduced with human PV (HPV)38 E6/E7 and human N/TERT cells or primary human keratinocytes (PHKs) were transduced with HPV8 E6, E7 or E6/E7; actin and tubulin were used as loading controls, respectively. (b) Lentiviral transduction of HeLa cells with CRISPR/Cas9 and specific guides for KRT17 created indels within the gene. Genomic sequences around the cut-sequences of HeLa K17KD (knockdown) cells were compared with the wildtype control using the ICE CRISPR analysis tool (Synthego, Redwood City, CA, USA) resulting in a calculated indel frequency (as a percentage) and a predicted knockout score. (c) Levels of *KRT17* mRNA were determined using reverse transcription-quantitative polymerase chain reaction (PCR). *HPRT1* was used as the reference gene. The mRNA levels of HeLa control cells (ctrl) were arbitrarily set to 1 [$n=4$, mean (SD), one-way ANOVA]. (b) Visualization of K17 in HeLa controls and HeLa K17KD cells. (e) Western blotting showed levels of cellular proteins in correlation to decreased K17 levels in HeLa K17KD cells in comparison with control cells. Vinculin was used as loading control. (f) In a pseudovirion-based infection assay, cells were infected with different dilutions of HPV18 pseudovirions delivering a luciferase reporter gene that allows a readout [mean (SD), $n=3$, one-way ANOVA]. (g) Levels of HPV18 *E6/E7* mRNA determined by quantitative PCR [mean (SD), $n=5$, one-way ANOVA]. (h) Levels of HPV18 E7 protein determined by Western blotting. Vinculin was used as loading control. ICE, Inference of CRISPR Edits; ns, not significant; PCAN, proliferating cell nuclear antigen.

PCNA (Figure 7e). Moreover, in line with the *in vivo* results (Figure S2), reduced K17 levels in HeLa KD cells resulted in increased levels of CD44 and CD271, two epithelial stemness markers.[13,35] Furthermore, correlated with the loss of K17, levels of active β-catenin were found to be increased while the amounts c-Myc were decreased (Figure 7e). Interestingly, both proteins were recently identified as regulatory proteins in MnPV-infected tissue in the proteomics approach.[26] These data suggest that loss of K17 affects important regulators of tissue homeostasis.

However, when subjecting the HeLa cells to a pseudovirion-based infection assay that allows quantifying infectivity rates by delivery of a luciferase reporter gene via HPV18 pseudovirions, no difference in susceptibility could be discerned (Figure 7f). Thus, K17 levels did not seem to affect viral entry into cells. Next, the effect of K17KD on HPV18 E6/E7 expression in the HeLa cells was assessed via qPCR, but no changes in expression of polycistronic E6/E7 transcripts could be detected (Figure 7 g). Conversely, Western blotting revealed a clear reduction of HPV18 E7 protein levels correlated to diminished K17 levels (Figure 7 h), pointing to post-transcriptional regulatory mechanisms affecting E7 protein levels.

Collectively, our data suggest that K17 expression is a common feature of tumorigenic skin. While it is not a primary target of PV oncoproteins, it may play a role in regulating viral protein synthesis.

Discussion

While K17 – with some exceptions (e.g. hair follicles) – is not expressed in normal tissues, it is induced upon keratinocyte proliferation during wound healing[3] and during growth of various tumours.[4–8] In the multistep process of SCC development, besides the major risk factor UV irradiation, PV infections are considered to play a cofactorial role.[11] However, it is unclear whether the presence of HPV in skin tumours depends on K17 expression or *vice versa.* Studies by Wang *et al.* initially suggested that MmuPV1 induces K17 as a novel host factor that supports viral persistence by modulating the cellular immune response,[30] but their further studies have more recently indicated that K17 supports viral persistence and tumour growth by modulating the local immune system.[57,58] Based on this proposed importance of K17 in PV-induced tumorigenesis, we have systematically studied K17 expression in skin tumours of different animal models and human tissues to further characterize its potential role in the viral life cycle. The high K17 levels not only in tumours from HPV-transgenic but also in HPV-unrelated skin tumours (Figure 1 and 2) suggests that PV presence does not contribute to K17 expression. This notion is supported by the results from MnPV-positive and -negative tumours from the *Mastomys* model (Figures 4 and S1), human premalignant lesions and SCCs (Figure 6) and various monolayer cell culture systems expressing PV oncoproteins (Figure 7a). Collectively, these data show that elevated K17 expression occurs independently of PV presence and is generally associated with cutaneous tumorigenesis.

In cutaneous SCCs, K17 loss can induce a less differentiated cellular state and increase stemness. This is in line with the observation that K17-positive areas in SCCs were costained for the epithelial marker E-cadherin, whereas areas positive for the mesenchymal marker vimentin were K17-negative (Figures S1 and S3). In the latter, viral persistence cannot be maintained,[25] putatively owing to the fact that PVs make use of the replication and gene expression machineries of more differentiated squamous cells.[59,60] Thus, although known as stress keratin, K17 may play a more fundamental role in skin homeostasis and tumour formation than commonly expected.

Tumours formed by HPV-positive SiHa K17KO and CaSki K17KO cells previously showed lower levels of S- and interphase markers[9] and exhibited slower growth or even spontaneous regression.[58] Indeed, as previously reported in different HeLa K17KO cells,[3] our two HeLa K17KD cell lines showed reduced proliferation as indicated by diminished PCNA levels (Figure 7e), correlated with the reduction of K17. Both HeLa K17KD cell lines showed increased levels of active β-catenin, CD44 and CD271 (Figure 7e), which are considered as cancer stem cell markers.[51,52,61] Conversely, c-Myc was found to be reduced upon K17KD, potentially fostering stem-like properties rather than an amplifying state.[62] Therefore, K17KD may keep the cell in a less differentiated state, thereby increasing the number of cells with stem-like characteristics. Particularly CD44 and CD271 were recently found to be upregulated in dedifferentiated areas of SCCs in the *Mastomys* model[26] and both CSC markers are linked to an EMT,[51] accompanied by a switch of E-cadherin and vimentin expression[31] and reduced expression of stress keratins (Table S2). Especially elevated CD271 levels in dedifferentiated SCC areas (Figure S2) point to the previously implied upregulated NGF signalling, which is linked to tumour growth and metastasis.[53,54]

In normal skin, K17 can only be found in the outer root sheath of hair follicles (Figure 2a and 3b),[63] which also contain follicular stem cells. Although such cells are considered to be the targets of PV virions during initial infection steps, we could not detect changes in susceptibility to PV virions when HeLa K17KD cells were compared with their wildtype cells (Figure 7f). Although K17KD did not influence viral gene transcription (Figure 7 g), viral E7 protein expression was found to be diminished (Figure 7 h), pointing to a regulatory mechanism downstream of transcription. K17KD causes a global reduction of protein synthesis,[3] which did not obviously affect CD44 and CD271 (Figure 7e). Further investigations may test whether the observed effect is excessively affecting PV proteins that would make K17 a restriction factor for HPV. For such studies, more suitable cell systems are desirable, as the HeLa/HPV18 system is not optimal for mimicking cutaneous PVs. Nevertheless, it allowed us to compare our results to previous studies, as many relevant *in vitro* experiments were previously performed in HeLa cells.[3] However, owing to the fact that PV replication and gene expression depends on the differentiation-dependent host cell machinery, it makes sense that diminished proliferation and protein synthesis in addition to unfavourable changes in the cellular differentiation state can abrogate viral persistence.

Anticipating K17 as a driver of tumorigenesis in general and as a factor involved in the control of viral gene expression, it may represent a target for therapy of both HPV-related and HPV-unrelated SCCs. Although many questions remain, our data exclude the possibility that PVs directly upregulate K17

expression during the development of epithelial tumours. Rather, K17 appears to create an environment that may be beneficial for viral maintenance.

Acknowledgements

We thank F. Rösl (DKFZ) for his support and for critically reading the manuscript despite his recent retirement. We kindly thank D. Viarisio (DKFZ) for providing tissue sections of HPV38 and HPV49 mice and K. Müller-Decker (DKFZ) for samples of DMBA/TPA-induced tumours. We further thank J. Doorbar (University of Cambridge) for generously providing anti-HPV8 E4 antibodies, K. Hoppe-Syler (DKFZ) for providing HPV18 E6/E7 primers and the HPV18 E7 antibody and M. Müller for providing HPV18 pseudovirions. We are grateful for the support and assistance by the animal technicians and veterinarians of the Center for Preclinical Research at the DKFZ is also gratefully acknowledged, with special thanks to K. Schmidt (Microbiological Diagnostics, DKFZ) for fruitful discussions and providing papilloma tissue of various transgenic mouse models observed during regular health checks. We further thank O. Kershaw (University of Berlin) for providing pathological reports for these specimens.

Funding sources

D.H. and I.B.-W. were supported by the Wilhelm Sander-Stiftung (grant numbers 2018.093.1 and 2018.093.2). S. Silling was supported by the National Reference Center for Papilloma- and Polyomaviruses (BMG Grant 1369-401). M.H. and B.A. were supported by the Deutsche Forschungsgemeinschaft (DFG, German Research Foundation, grant number 502233329).

Conflicts of interest

The authors declare no conflicts of interest. D.H. is currently working at the BioNTech SE. All work presented here was generated before D.H. joined BioNTech SE and is not related to BioNTech SE.

Data availability

The data underlying this article are available in the article and in its online supplementary material.

Ethics statement

The animals were housed and handled in accordance with local (DKFZ), German and European statutes. Experiments were approved by responsible Animal Ethics Committee for the use and care of live animals (Regional Council of Karlsruhe, Germany, file nos. G26/12 and G289/15). Clinical specimens were included from a series of tissue samples obtained between September and November 2021 by excision surgery. The study was approved by the Ethical Committee of the University Witten/Herdecke, Germany (reference no. 166/2017).

Patient consent

Written patient consent for publication was obtained.

Supporting Information

Additional Supporting Information may be found in the online version of this article at the publisher's website.

References

1 Ho M, Thompson B, Fisk JN *et al.* Update of the keratin gene family: evolution, tissue-specific expression patterns, and relevance to clinical disorders. *Hum Genomics* 2022; **16**:1.
2 Yang L, Zhang S, Wang G. Keratin 17 in disease pathogenesis: from cancer to dermatoses. *J Pathol* 2019; **247**:158–65.
3 Kim S, Wong P, Coulombe PA. A keratin cytoskeletal protein regulates protein synthesis and epithelial cell growth. *Nature* 2006; **441**:362–5.
4 Merkin RD, Vanner EA, Romeiser JL *et al.* Keratin 17 is overexpressed and predicts poor survival in estrogen receptor-negative/human epidermal growth factor receptor-2-negative breast cancer. *Hum Pathol* 2017; **62**:23–32.
5 Roa-Peña L, Leiton CV, Babu S *et al.* Keratin 17 identifies the most lethal molecular subtype of pancreatic cancer. *Sci Rep* 2019; **9**:11239.
6 Ujiie D, Okayama H, Saito K *et al.* KRT17 as a prognostic biomarker for stage II colorectal cancer. *Carcinogenesis* 2020; **41**:591–9.
7 Regenbogen E, Mo M, Romeiser J *et al.* Elevated expression of keratin 17 in oropharyngeal squamous cell carcinoma is associated with decreased survival. *Head Neck* 2018; **40**:1788–98.
8 Escobar-Hoyos LF, Yang J, Zhu J *et al.* Keratin 17 in premalignant and malignant squamous lesions of the cervix: proteomic discovery and immunohistochemical validation as a diagnostic and prognostic biomarker. *Mod Pathol* 2014; **27**:621–30.
9 Escobar-Hoyos LF, Shah R, Roa-Peña L *et al.* Keratin-17 promotes p27KIP1 nuclear export and degradation and offers potential prognostic utility. *Cancer Res* 2015; **75**:3650–62.
10 Leblebici C, Pasaoglu E, Kelten C *et al.* Cytokeratin 17 and Ki-67: immunohistochemical markers for the differential diagnosis of keratoacanthoma and squamous cell carcinoma. *Oncol Lett* 2017; **13**:2539–48.
11 Hasche D, Vinzón SE, Rösl F. Cutaneous papillomaviruses and non-melanoma skin cancer: causal agents or innocent bystanders? *Front Microbiol* 2018; **9**:874.
12 Gheit T. Mucosal and cutaneous human papillomavirus infections and cancer biology. *Front Oncol* 2019; **9**:355.
13 Hufbauer M, Maltseva M, Meinrath J *et al.* HPV16 increases the number of migratory cancer stem cells and modulates their miRNA expression profile in oropharyngeal cancer. International journal of cancer. *Int J Cancer* 2018; **143**:1426–39.
14 Hubbers CU, Akgül B. HPV and cancer of the oral cavity. *Virulence* 2015; **6**:244–8.
15 Smola S. Human papillomaviruses and skin cancer. *Adv Exp Med Biol* 2020; 1268:195–209.
16 Hufbauer M, Akgül B. Molecular mechanisms of human papillomavirus induced skin carcinogenesis. *Viruses* 2017; **9**:187.
17 Schaper ID, Marcuzzi GP, Weissenborn SJ *et al.* Development of skin tumors in mice transgenic for early genes of human papillomavirus type 8. *Cancer Res* 2005; **65**:1394–400.
18 Hufbauer M, Cooke J, van der Horst GT *et al.* Human papillomavirus mediated inhibition of DNA damage sensing and repair drives skin carcinogenesis. *Mol Cancer* 2015; **14**:183.
19 Heuser S, Hufbauer M, Steiger J *et al.* The fibronectin/α3β1 integrin axis serves as molecular basis for keratinocyte invasion induced by βHPV. *Oncogene* 2016; **35**:4529–39.
20 Viarisio D, Müller-Decker K, Accardi R *et al.* Beta HPV38 oncoproteins act with a hit-and-run mechanism in ultraviolet radiation-induced skin carcinogenesis in mice. *PLOS Pathog* 2018; **14**:e1006783.

21 Viarisio D, Müller-Decker K, Zanna P *et al.* Novel ß-HPV49 transgenic mouse model of upper digestive tract cancer. *Cancer Res* 2016; **76**:4216–25.
22 Zhussupbekova S, Sinha R, Kuo P *et al.* A mouse model of hyperproliferative human epithelium validated by keratin profiling shows an aberrant cytoskeletal response to injury. *EBioMedicine* 2016; **9**:314–23.
23 Hasche D, Rösl F. *Mastomys* species as model systems for infectious diseases. *Viruses* 2019; **11**:182.
24 Ahmels M, Mariz FC, Braspenning-Wesch I *et al.* Next generation L2-based HPV vaccines cross-protect against cutaneous papillomavirus infection and tumor development. *Front Immunol* 2022; **13**:1010790.
25 Hasche D, Stephan S, Braspenning-Wesch I *et al.* The interplay of UV and cutaneous papillomavirus infection in skin cancer development. *PLOS Pathog* 2017; **13**:e1006723.
26 Schäfer M, Schneider M, Müller T *et al.* Spatial tissue proteomics reveals distinct landscapes of heterogeneity in cutaneous papillomavirus-induced keratinocyte carcinomas. *J Med Virol* 2023; **95**:e28850.
27 Weissenborn SJ, Nindl I, Purdie K *et al.* Human papillomavirus-DNA loads in actinic keratoses exceed those in non-melanoma skin cancers. *J Invest Dermatol* 2005; **125**:93–7.
28 Hu J, Cladel NM, Budgeon LR *et al.* The mouse papillomavirus infection model. *Viruses* 2017; **9**:246.
29 Spurgeon ME, Lambert PF. Sexual transmission of murine papillomavirus (MmuPV1) in *Mus musculus*. *eLife* 2019; **8**:e50056.
30 Wang W, Uberoi A, Spurgeon M *et al.* Stress keratin 17 enhances papillomavirus infection-induced disease by downregulating T cell recruitment. *PLOS Pathog* 2020; **16**:e1008206.
31 Hasche D, Ahmels M, Braspenning-Wesch I *et al.* Isoforms of the papillomavirus major capsid protein differ in their ability to block viral spread and tumor formation. *Front Immunol* 2022; **13**:811094.
32 Gebhardt C, Riehl A, Durchdewald M *et al.* RAGE signaling sustains inflammation and promotes tumor development. *J Exp Med* 2008; **205**:275–85.
33 de Koning M, Quint W, Struijk L *et al.* Evaluation of a novel highly sensitive, broad-spectrum PCR-reverse hybridization assay for detection and identification of beta-papillomavirus DNA. *J Clin Microbiol* 2006; **44**:1792–800.
34 Akgül B, Bauer B, Zigrino P *et al.* Upregulation of lipocalin-2 in human papillomavirus-positive keratinocytes and cutaneous squamous cell carcinomas. *J Gen Virol* 2011; **92**:395–401.
35 Schäfer K, Neumann J, Waterboer T, Rösl F. Serological markers for papillomavirus infection and skin tumour development in the rodent model *Mastomys coucha*. *J Gen Virol* 2011; **92**:383–94.
36 Panchal NK, Bhale A, Chowdary R *et al.* PCR amplifiable DNA from breast disease FFPE section for mutational analysis. *J Biomol Tech* 2020; **31**:1–6.
37 Dickson MA, Hahn WC, Ino Y *et al.* Human keratinocytes that express hTERT and also bypass a p16(INK4a)-enforced mechanism that limits life span become immortal yet retain normal growth and differentiation characteristics. *Mol Cell Biol* 2000; **20**:1436–47.
38 Montague TG, Cruz JM, Gagnon J *et al.* CHOPCHOP: a CRISPR/Cas9 and TALEN web tool for genome editing. *Nucleic Acid Res* 2014; **42**:W401–7.
39 Hsu PD, Scott DA, Weinstein JA *et al.* DNA targeting specificity of RNA-guided Cas9 nucleases. *Nat Biotechnol* 2013; **31**:827–32.
40 Revia S, Seretny A, Wendler L *et al.* Histone H3K27 demethylase KDM6A is an epigenetic gatekeeper of mTORC1 signalling in cancer. *Gut* 2022; **71**:1613–28.
41 Conant D, Hsiau T, Rossi N *et al.* Inference of CRISPR edits from Sanger trace data. *CRISPR J* 2022; **5**:123–30.
42 Hufbauer M, Biddle A, Borgogna C *et al.* Expression of betapapillomavirus oncogenes increases the number of keratinocytes with stem cell-like properties. *J Virol* 2013; **87**:12158–65.
43 Akgül B, Ghali L, Davies D *et al.* HPV8 early genes modulate differentiation and cell cycle of primary human adult keratinocytes. *Exp Dermatol* 2007: **16**:590–9.
44 Akgül B, Garcia-Escudero R, Ghali L *et al.* The E7 protein of cutaneous human papillomavirus type 8 causes invasion of human keratinocytes into the dermis in organotypic cultures of skin. *Cancer Res* 2005; **65**:2216–23.
45 Akgül B, Kirschberg M, Storey A, Hufbauer M. Human papillomavirus type 8 oncoproteins E6 and E7 cooperate in downregulation of the cellular checkpoint kinase-1. *Int J Cancer* 2019; **145**:797–806.
46 Vinzón SE, Braspenning-Wesch I, Müller M *et al.* Protective vaccination against papillomavirus-induced skin tumors under immunocompetent and immunosuppressive conditions: a preclinical study using a natural outbred animal model. *PLOS Pathog* 2014; **10**:e1003924.
47 Fu Y, Cao R, Schäfer M *et al.* Expression of different L1 isoforms of *Mastomys natalensis* papillomavirus as mechanism to circumvent adaptive immunity. *eLife* 2020; **9**:e57626.
48 Sehr P, Rubio I, Seitz H *et al.* High-throughput pseudovirion-based neutralization assay for analysis of natural and vaccine-induced antibodies against human papillomaviruses. *PLOS ONE* 2013; **8**:e75677.
49 Dongre A, Weinberg RA. New insights into the mechanisms of epithelial-mesenchymal transition and implications for cancer. *Nat Rev Mol Cell Biol* 2019; **20**:69–84.
50 Batlle E, Clevers H. Cancer stem cells revisited. *Nature Med* 2017; **23**:1124–34.
51 Elkashty, OA, Abu Elghanam G, Su X *et al.* Cancer stem cells enrichment with surface markers CD271 and CD44 in human head and neck squamous cell carcinomas. *Carcinogenesis* 2020; **41**:458–66.
52 Strohmayer C, Klang A, Kummer S *et al.* Tumor cell plasticity in equine papillomavirus-positive versus-negative squamous cell carcinoma of the head and neck. *Pathogens* 2022; **11**:266.
53 Redmer T, Welte Y, Behrens D *et al.* The nerve growth factor receptor CD271 is crucial to maintain tumorigenicity and stem-like properties of melanoma cells. *PLOS ONE* 2014; **9**:e92596.
54 Wu R, Li K, Yuan M, Luo KQ. Nerve growth factor receptor increases the tumor growth and metastatic potential of triple-negative breast cancer cells. *Oncogene* 2021; **40**:2165–81.
55 Nafz J, Ohnesorge M, Stockfleth E *et al.* Imiquimod treatment of papilloma virus and DMBA/TPA-induced cutaneous skin cancer in *Mastomys coucha*: an unique animal model system useful for preclinical studies. *Br J Dermatol* 2007; **157** (Suppl. 2):14–17.
56 Hasche D, Stephan S, Savelyeva L *et al.* Establishment of an immortalized skin keratinocyte cell line derived from the animal model *Mastomys coucha*. *PLOS ONE* 2016; **11**:e0161283.
57 Wang W, Spurgeon ME, Pope A *et al.* Stress keratin 17 and estrogen support viral persistence and modulate the immune environment during cervicovaginal murine papillomavirus infection. *Proc Natl Acad Sci USA* 2023; **120**:e2214225120.
58 Wang W, Lozar T, Golfinos AE *et al.* Stress keratin 17 expression in head and neck cancer contributes to immune evasion and resistance to immune-checkpoint blockade. *Clin Cancer Res* 2022; **28**:2953–68.
59 Graham SV. Keratinocyte differentiation-dependent human papillomavirus gene regulation. *Viruses* 2017; **9**:245.
60 Doorbar J, Egawa N, Griffin H *et al.* Human papillomavirus molecular biology and disease association. *Rev Med Dermatol* 2015; **25** (Suppl. 1): 2–23.
61 Zhou HM, Zhang JG, Zhang X, Li Q. Targeting cancer stem cells for reversing therapy resistance: mechanism, signaling, and prospective agents. *Signal Transduct Target Ther* 2021; **6**:62.
62 Arnold I, Watt FM. c-Myc activation in transgenic mouse epidermis results in mobilization of stem cells and differentiation of their progeny. *Curr Biol* 2001; **11**:558–68.
63 Kurokawa I, Takahashi K, Moll I, Moll R. Expression of keratins in cutaneous epithelial tumors and related disorders – distribution and clinical significance. *Exp Dermatol* 2011; **20**:217–28.